Nonlinear Digital Self-Interference Cancellation with Reduced Complexity for Full Duplex Systems

Mustafa Emara*†, Kilian Roth*†, Leonardo G. Baltar*, Michael Faerber*, Josef A. Nossek†‡
* Next Generation and Standards, Intel Deutschland GmbH, Neubiberg, Germany
Email: {Mustafa.emara, Kilian.roth, Leo.baltar, Michael.faerber}@intel.com
† Department of Electrical and Computer Engineering, Technical University Munich, Munich, Germany
‡ Department of Teleinformatics Engineering, Federal University of Ceara, Fortaleza, Brazil
Email: {Mostafa.Talat, Kilian.roth, Josef.a.nossek}@tum.de

***Abstract*—Full duplex transmission is currently viewed as an important technology component for the future 5G and beyond mobile broadband technology. In order to realize its promised theoretical gain, sufficient cancellation of the self-interference must be achieved. The focus throughout this work will be on the digital cancellation, which main target is to cancel the residual self-interference resulting from the insufficient analog cancellation due to hardware imperfections, along with non-linearities existing in the transmitter chain. A novel pre-transmission transformation based on the Cholesky decomposition is presented, that aims at enhancing the digital cancellation performance. A digital cancellation based on the transversal recursive least squares with the exploitation of the dichotomous coordinate descent algorithm to lower the computational complexity is presented. The analysis was extended to include the existence of a received signal of interest, while simultaneously canceling the self-interference signal. By means of numerical simulations, a performance evaluation was carried out and results showed that the level of residual interference after the digital canceler reaches the simulated noise floor power level.**

I. Introduction

THE wireless future industry including 5G and beyond will be prominent by an extensive wireless integration of smartphones, wearables, sensors, tablets, drones and other objects into a massive integrated system [1]. Realizing the requirements for an incorporation of users within such a diverse pool implies a paradigm shift of the spectrum utilization. The current research has been directed into spectrally efficient transmission schemes to cope with the unprecedented volume of data [2]. Among the investigated topics are the full-duplex transmission schemes [3]–[5]. Theoretically, full-duplex transmission allows the full utilization of the available resources in both transmission directions downlink and uplink, thus, leading to doubling the achievable rates [6].

In order to realize the full-duplex gains, sufficient cancellation of the self-interference (SI) should be carried out. The main bottleneck is the large power difference between SI signal resulting from a device's own wireless transmissions and the received signal of interest (SoI) coming from a distant transmitting node [5]. The SI cancellation is carried over three main stages: passive, analog and digital cancellation. The focus of this paper is the digital cancellation, which aims at canceling the residual SI after the analog and passive cancellation along with the cancellation of the nonlinearities existing in the transmitter chain [5]. The digital cancellation plays an important role to further cancel the SI signal down to the noise floor level in order to provide a success reception of the received SoI.

Different schemes for the digital canceler in full duplex systems have been covered over the past years in the literature. In [7], an extension of the purely digital approach towards including an additional receiving chain has been introduced. The main drawback of this architecture are the hardware limitations, mainly, the low noise amplifier (LNA) saturation of the Rx chain. Another approach was presented in [8], where a joint and successive iterative estimation of the channel and nonlinear coefficients was adopted. Although it provides high cancellation performance, orthogonal training sequence and dependency on a specific waveform were the main problems with this solution. Another joint estimation solution was introduced in [9] which exploits the common phase error cancellation. The main constraint is the requirement for high-resolution channel estimates and signal-to-noise-ratio (SNR) values at the receiver. A more recent adaptive algorithm was introduced in [10] which was based on the nonlinear adaptive estimation of the SI channel and iteratively computing the SI channel. The main limitation of the mentioned technique is the tuning required for the adaptation algorithm and the performance limitations imposed by the digital canceler. The proposed algorithm throughout this contribution aims to solve those two mentioned problems by providing high cancellation performance with low computational complexity.

This work is organized as follows: Section II presents the system and the signal model used. Afterwards, a pre-estimation process based on the transformation of the power functions along with the proposed cancellation algorithm are explained in Section III. Furthermore, the simulation results are presented and explained in Section IV. Finally, a summary is provided in Section V.

II. Signal Model

The system model investigated through this work is shown in Fig. 1. The generated baseband transmitted signal denoted by $x[n]$ first gets passed through the transmitter front-end, resulting in the analog signal at the power amplifier (PA) output $x_{\text{PA}}(t)$. Afterwards, the signal propagates through a

ISBN 978-3-8007-4394-0

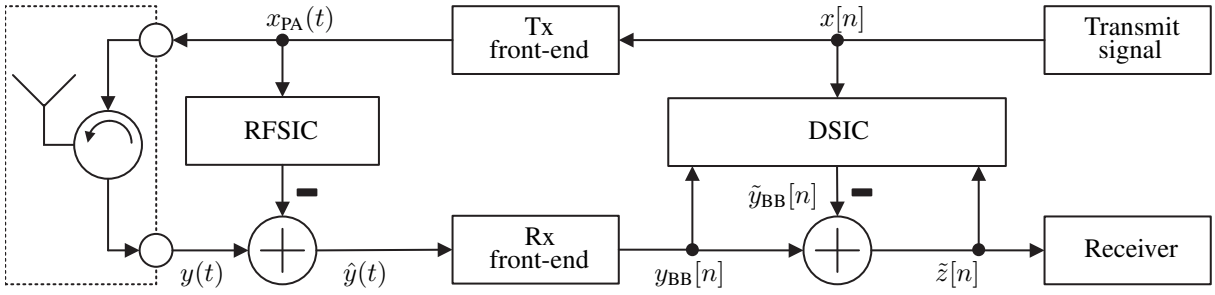

Fig. 1. System model of the investigated full duplex system.

circulator for transmission. In the investigated architecture, a single antenna for transmission and reception is utilized. As a result, a circulator is required to separate between the the transmission and reception directions [5]. The received signal denoted by $y(t)$, includes the SoI along with the SI signal. At this stage, the received signal is subjected to the radio frequency self-interference cancellation (RFSIC) stage, where $\hat{y}(t)$ is the signal after the RFSIC. The objective of the RFSIC is to create a replica of the analog transmitted signal and then subtract it from the received signal. The resulted signal $\hat{y}(t)$ is then processed by the receiver's hardware, resulting in the digital baseband signal $y_{\text{BB}}[n]$, which incorporates the residual linear, nonlinear SI and the received SoI. The digital self-interference cancellation (DSIC) block is then utilized to compute an estimate of the SI signal denoted by $\tilde{y}_{\text{BB}}[n]$, which is subtracted from the actual SI signal resulting in the received residual signal $\tilde{z}[n]$ after the digital cancellation stage.

The primary focus will be on modeling the SI signal present in the transceiver's chain. For a highly nonlinear PA, different models have been extensively studied throughout the literature [11]. The Volterra series provides a general model with memory. Its main drawback is the large complexity cost due to the large number of coefficients to be estimated [12]. As a result, the focus has shifted to Volterra variants, specifically the Hammerstein model [13]. This model incorporates a static non-linearity followed by a linear time invariant filter. The static nonlinearity was chosen as the power polynomial function that originates from a power series expansion [14].

As demonstrated in Figure 1, the generated transmitted signal goes first through the Tx chain and then propagates through the circulator and is convolved with the SI channel. The SI channel represents the channel experienced by the signal after at the PA output till the input of the RFSIC. The main components of the SI channel are the reflections due to antenna mismatching and leakage through the circulator [15]. Following the assumption that the PA dominates the nonlinearities existent in the SI signal [16], and considering the SI channel as a linear time invariant system, the signal can be modeled using a Hammerstein model [12]. Furthermore, the DSIC block can be built as a nonlinear system followed by a linear system. As a result, this block represents another Hammerstein model. Accordingly, the overall SI baseband signal can be represented using a parallel Hammerstein model as follows

$$\begin{aligned} y_{\text{BB}}[n] &= \sum_{m=0}^{M-1} \sum_{p=1}^{P} h_p[m] \phi_p(x[n-m]), \\ \phi_p(x[n]) &= x[n]|x[n]|^{p-1}, \end{aligned} \tag{1}$$

where M is the memory depth of the model and $P-1$ is the nonlinearity polynomial order. Additionally, $h_p[m]$ is the p-th order channel coefficients of the effective SI channel and $\phi_p(x[n])$ denotes the nonlinear basis function of the baseband signal $x[n]$. In order to provide a sufficient level of digital cancellation, precise estimation of $h_p[m]$ is necessary. Denoting the estimated SI channel coefficients by $\tilde{h}_p[m]$, the received SoI by $r_{\text{SoI}}[n]$ and the additive white Gaussian noise (AWGN) in the receiver's chain by $\eta[n]$, the residual SI after digital cancellation is

$$\begin{aligned} \tilde{z}[n] =& r_{\text{SoI}}[n] + \eta[n] + y_{\text{BB}}[n] - \tilde{y}_{\text{BB}}[n], \\ =& r_{\text{SoI}}[n] + \eta[n] \\ &+ \underbrace{y_{\text{BB}}[n] - \sum_{m=0}^{M-1} \sum_{p=1}^{P} \tilde{h}_p[m] \phi_p(x[n-m])}_{\text{Residual SI}}. \end{aligned} \tag{2}$$

Throughout this work, efficient algorithms for estimating $\tilde{h}_p[m]$ will be presented. Furthermore, the cancellation performance and the computational complexity represent the main key peformance indicators (KPI) in this work.

III. Digital Self-Interference Cancellation

A. Basis Functions Transformation

As mentioned earlier, the basis function $\phi_p(x[n])$ represent the nonlinear modeling of the transmitted baseband signal $x[n]$ for a given nonlinearity order p. Since we generate P nonlinear basis functions for every incoming sample, the basis functions across different nonlinearity orders are highly correlated. As a result, slow convergence and a degraded cancellation process is achieved when finding the optimum estimation of the SI effective channel coefficients. Consequently, an orthogonalization of the basis functions before the coefficients estimation

ISBN 978-3-8007-4394-0

is required [17]. The covariance matrix of the basis functions across sufficiently large number of samples can be computed as follows

$$\boldsymbol{\Upsilon} = \mathbb{E}[\boldsymbol{\phi}[n]\boldsymbol{\phi}^{\mathrm{H}}[n]], \tag{3}$$

where $\mathbb{E}[\cdot]$ is the expectation operation and $\boldsymbol{\phi}[n]$ is the instantaneous basis functions for the n-th sample and is defined as $\boldsymbol{\phi}[n] = [\phi_1[n]\ \phi_2[n] \dots \phi_P[n]]^{\mathrm{T}}$. Afterwards, a transformation of the basis function is carried out via a whitening transformation matrix $\boldsymbol{T}$ based on the Cholesky decomposition as follows

$$\begin{aligned} \boldsymbol{\Upsilon} &= \boldsymbol{L}\boldsymbol{L}^{\mathrm{H}}, \\ \boldsymbol{T} &= \boldsymbol{L}^{-1}, \end{aligned} \tag{4}$$

where $\boldsymbol{L}$ is a lower triangular matrix with positive diagonal entries. Assuming the knowledge of the transmitted signal statistics, the matrix $\boldsymbol{T}$ can be computed offline and used on the fly. Furthermore, it can be computed independent of the transmitted signal, only following the assumption that the baseband symbols can be well approximated by a Gaussian distribution. This assumption is valid for the class of multi-carrier waveforms (orthogonal frequency division multiplexing (OFDM) based or filter bank multi-carrier (FBMC)). Thus, $x[n]$ can be approximated by a circular symmetric complex Gaussian variable with unit variance and zero mean. For the non-orthogonal basis functions, the expectation of the l-th and the m-th components follows

$$\mathbb{E}[\phi_l[n]\phi_m[n]] \neq 0, \ \ \forall \ l, m \in \{1, 2, \cdots, P\}. \tag{5}$$

Additionally, by employing the definition of $\phi_p[n]$ as in (1), equation (eq:corrlm) can be rewritten as

$$\begin{aligned} \mathbb{E}[\phi_l[n]\phi_m[n]] &= \mathbb{E}[x[n]|x[n]|^{l-1}x^*[n]|x[n]|^{m-1}], \\ &= \mathbb{E}[|x[n]|^{l+m}]. \end{aligned} \tag{6}$$

Following the assumption that $x[n]$ is Gaussian with unit variance, the covariance computation solution can be simplified for $l, m \in \{1, 2, \cdots, P\}$ as follows

$$\mathbb{E}[|x[n]|^{l+m}] = \tag{7}$$

$$\begin{cases} \frac{l+m}{2}!, & l+m \text{ even} \\ (\frac{1}{2})^{\frac{l+m+1}{2}}\sqrt{\pi}\prod_{i=0}^{\frac{l+m-1}{2}}(2i+1), & l+m \text{ odd} \end{cases} \tag{8}$$

Accordingly, the orthogonalized basis functions $\tilde{\boldsymbol{\phi}}[n]$ are computed as follows

$$\tilde{\boldsymbol{\phi}}[n] = \boldsymbol{T}\boldsymbol{\phi}[n]. \tag{9}$$

In order to better rewrite the signal model, (2) can be reformulated such that the data vector for the previous M samples are included as

$$\boldsymbol{u}[n] = [\tilde{\boldsymbol{\phi}}^{\mathrm{T}}[n]\ \tilde{\boldsymbol{\phi}}^{\mathrm{T}}[n-1] \dots \tilde{\boldsymbol{\phi}}^{\mathrm{T}}[n-M+1]]^{\mathrm{T}}, \tag{10}$$

where $\boldsymbol{u}[n]$ is the input complex data vector and $\boldsymbol{u}[n] \in \mathbb{C}^{MP\times 1}$. Applying the same notation to the estimated SI channel coefficients $\tilde{\boldsymbol{h}}[n]$ can be written as

$$\tilde{\boldsymbol{h}}[n] = [\tilde{h}_1[n]\ \tilde{h}_2[n] \dots \tilde{h}_P[n] \dots \tilde{h}_P[n-M+1]]^{\mathrm{T}}, \tag{11}$$

where $\tilde{\boldsymbol{h}}[n]$ are the SI channel coefficient to be estimated and $\tilde{\boldsymbol{h}}[n] \in \mathbb{C}^{MP\times 1}$. Finally, by plugging (10) and (11) into (2), the residual SI cancellation can be denoted by

$$\tilde{z}[n] = r_{SoI}[n] + \eta[n] + y_{\mathrm{BB}}[n] - \tilde{\boldsymbol{h}}^{\mathrm{H}}[n]\boldsymbol{u}[n]. \tag{12}$$

Throughout the next subsection, an efficient cancellation algorithm will be presented based on the precise estimation and tracking of the SI channel coefficients $\tilde{\boldsymbol{h}}[n]$.

B. Self-Interference Channel Estimation

The DSIC objective is to exploit the available baseband data at the transmitter in order to regenerate the SI signal and subtract it from the actual received SI samples. Throughout this paper, a suggested Recursive least squares (RLS) algorithm combined with complexity reduction technique is proposed to be deployed at the digital canceler for full-duplex systems.

The RLS algorithm chosen in this work deals with solving the auxiliary formulation of the least squares problem [18]. The summary of the proposed exponentially weighted RLS is presented in Table I. An initialization step is first conducted before transmission, where the residual vector $\boldsymbol{r}[n]$ is set to the covariance vector $\boldsymbol{\beta_o}[n]$. The correlation matrix $\boldsymbol{R}[n]$ is set to an equalization matrix $\boldsymbol{\Pi}$, which is defined as $\boldsymbol{\Pi} = \alpha\boldsymbol{I}_{MP}$, where $\boldsymbol{I}_{MP}$ is an identity matrix of dimension $MP \times MP$ and α is chosen based on the SNR as $0 < \alpha < 1$ [19]. The parameter λ is the forgetting factor that is chosen as $0 << \lambda \leq 1$. The first step represents the update of the correlation matrix for each incoming sample. Originally, the update should consider all the incoming input data vector $\boldsymbol{u}[n]$. Nevertheless, following the stationarity assumption of the input data, only the first p components of the data vector are sufficient to reconstruct the complete correlation matrix. Those p components are fully captured in $\tilde{\boldsymbol{\phi}}[n]$. Accordingly, $\boldsymbol{R}^{(1:p)}[n]$ represents the first p rows of the correlation matrix. Thus, by exploring the transversal structure of the input data vector, a reduction in the computational complexity can be achieved.

Such a reformulation of the RLS problem was utilized to provide a reduced computational complexity compared to that of the conventional RLS algorithm in [19]. In order to realize a reduced computational complexity, efficient solution should be utilized to solve step 4, which constitutes the complexity bottleneck of the algorithm. This step results in computing the coefficients update $\Delta\tilde{\boldsymbol{h}}[n]$ along with the residual vector $\boldsymbol{r}[n]$. Furthermore, P_M and P_A stand for the complexity of real multiplications and additions respectively. The conjugate gradient and coordinate descent are examples of exact line search algorithms [18], [20]. High convergence speed can be achieved by the conjugate gradient method [20]. However, its complexity is a limiting factor as it requires a complexity of $\mathcal{O}((MP)^2)$ per sample, which is too high for the targeted KPI of our digital canceler for practical implementations. A less complex solution is obtained with the coordinate descent algorithm [18], which achieves as well high cancellation results, but requires MP multiplications. As a result, the focus

ISBN 978-3-8007-4394-0

TABLE I
EXPONENTIALLY RECURSIVE LEAST MEAN SQUARES ALGORITHM

Step	Computation	real x	real +
	Intialization: $\tilde{\boldsymbol{h}}[0]=\boldsymbol{0}, \tilde{z}[0]=0$ $\boldsymbol{r}[0]=\boldsymbol{0}, \boldsymbol{R}[0]=\boldsymbol{\Pi}$		
	while transmitting $(n \geq 1)$	-	-
1	$\boldsymbol{R}^{(1:p)}[n]=\lambda \boldsymbol{R}^{(1:p)}[n-1]+\tilde{\boldsymbol{\phi}}[n]\boldsymbol{u}^{\mathrm{H}}[n]$	$6MP^2$	$4MP^2$
2	$\tilde{z}[n]=y_{\mathrm{BB}}[n]-\tilde{\boldsymbol{h}}^{\mathrm{H}}[n-1]\boldsymbol{u}[n]$	$4MP$	$2(MP+1)$
3	$\boldsymbol{\beta_o}[n]=\lambda \boldsymbol{r}[n-1]+\tilde{z}^{*}[n]\boldsymbol{u}[n]$	$6MP$	$4MP$
4	$\boldsymbol{R}[n]\Delta\tilde{\boldsymbol{h}}[n]=\boldsymbol{\beta_o}[n] \Rightarrow \Delta\tilde{\boldsymbol{h}}[n], \boldsymbol{r}[n]$	P_M	P_A
5	$\tilde{\boldsymbol{h}}[n]=\tilde{\boldsymbol{h}}[n-1]+\Delta\tilde{\boldsymbol{h}}[n]$	-	$2MP$
	Total: $\times: 6MP^2+10(MP)+P_M$ Total $+: 4MP^2+8MP+2+P_A$	-	-

of this work is towards the dichotomous coordinate descent (DCD) algorithm due to its advantage of low complexity [21].

The main motivation of the DCD algorithm is to avoid multiplications, divisions and square roots while solving the system of linear equations. This can be achieved through modifying the coordinate descent algorithm [18]. The detailed steps of the DCD algorithm are presented in Algorithm 1. The step-size μ of the solution is quantized and assigned a distinct value out of M_b possible values, where M_b is the number of bits used for the binary representation of $\Delta\tilde{\boldsymbol{h}}[n]$. Additionally, the range $[-\kappa,\ \kappa]$, where κ is the maximum amplitude of $\tilde{\boldsymbol{h}}[n]$ and represents the dynamic range of the targeted solution.

The algorithm considers finding iteratively the solution for the most significant bit and then moves to a less significant bit and so forth until all the bits are handled. Due to step-size quantization, the solution $\Delta\tilde{\boldsymbol{h}}[n]$ and the residual vector $\boldsymbol{r}[n]$ are updated based on the condition $|\boldsymbol{r}_k| > (\mu/2)[\boldsymbol{R}]_{k,k}$, where $[\boldsymbol{R}]_{k,k}$ is the element in the k-th row and k-th column of the correlation matrix $\boldsymbol{R}$. If the condition is satisfied, the iteration is labeled as a successful iteration, otherwise, as an unsuccessful one. For successful iterations, the residual vector and the step coefficients are updated. The notation $\boldsymbol{R}^{(k)}$ denotes the kth column of the correlation matrix. Additionally, the parameter N_u defines the number of iterations that needs to be conducted on every element of the filter weights.

It has been shown in [18] that for the worst case scenario, the maximum number of additions P_A required is upper bounded by $N(2N_u+M_b-1)+N_u$. As a result, the number of real multiplications of the proposed transversal RLS algorithm is $6MP^2+10(MP)$.

IV. NUMERICAL RESULTS

In this section, the simulation results for the discussed concepts in the previous sections are presented. The main simulation parameters are presented in Table II. Throughout this work, behavioural modeling was considered for the different hardware components of the transceiver's chain [22]. As mentioned in Section II, the choice of the PA model affects the overall system nonlinearities. The power series model, or the polynomial model, until the 5-th coefficient was considered for the PA model. Additionally, the two key performance indicators that will be investigated are the cancellation performance and the computational complexity. The latter represents the practicality of the proposed algorithms with limited hardware resources. The studied Tx signal is based on OFDM modulation.

In Figure 2,the power spectrum density (PSD) of the residual SI power is showed at three main stages: PA output, after RFSIC and after DSIC. The signal power was normalized to the transmitter signal power in order to ease the visualization of the cancellation performance. The SI is first attenuated in the analog domain using the circulator and the analog canceler. A combined cancellation value of $\approx$ 50 dB is achieved in the analog domain. It can be observed in the PSD plot the effect of the selectivity of the SI channel. Throughout this work, the RFSIC was modeled using an finite impulse response (FIR) filter to provide the required linear SI cancellation. Further cancellation of the residual linear and the nonlinear components is carried out by the digital canceler.

Algorithm 1 Dichotomous coordinate descent

Initialization: $\Delta\tilde{\boldsymbol{h}}=\boldsymbol{0}$, $\boldsymbol{r}=\boldsymbol{\beta}_o$, $m=0$, $k=0$, $\mu=\kappa$
while $m \leq M_b$ **do**
  $\mu \leftarrow \mu/2$
  flag $\leftarrow 0$
  while $k \leq MP$ **do**
    if $|\boldsymbol{r}_k| > (\mu/2)[\boldsymbol{R}]_{k,k}$ **then**
      $\Delta\tilde{\boldsymbol{h}}_k \leftarrow \Delta\tilde{\boldsymbol{h}}_k + \mathrm{sign}(\boldsymbol{r}_k)\mu$
      $\boldsymbol{r}_k \leftarrow \boldsymbol{r}_k - \mathrm{sign}(\boldsymbol{r}_k)\mu\boldsymbol{R}^{(k)}$
      $q \leftarrow q+1$, flag $\leftarrow 1$
      if $q > N_u$ **then Return**
      end if
    end if
    $k \leftarrow k+1$
  end while
  if flag = 1 **then** flag $\leftarrow 0$, **go to** step 5
  $m \leftarrow m+1$
end while

TABLE II
SIMULATION PARAMETERS FOR THE FULL-DUPLEX SIMULATOR

Parameter	value
Noise floor	-90 dBm
Received signal power	-80 dBm
Bandwidth	20 MHz
Circulator isolation	20 dB
Memory depth (M)	10
Nonlinearity order $(P-1)$	4
Forgetting factor (λ)	0.9
Number of updates iterations (N_u)	1
Bits for binary representation (M_b)	8
DCD maximum weight update (κ)	2^{-9}

ISBN 978-3-8007-4394-0

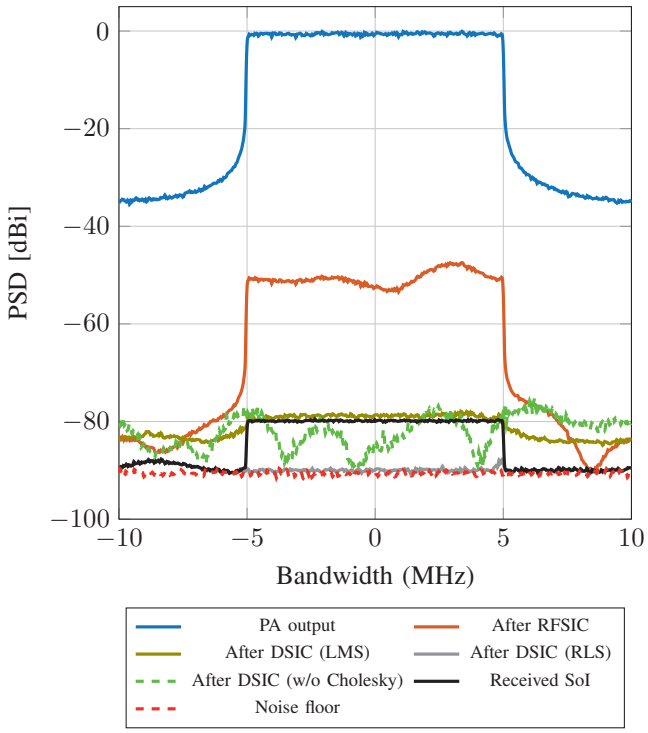

Fig. 2. Cancellation Performance in the presence of received signal of interest.

The first algorithm is based on the least mean squares (LMS) algorithm, which represents the state-of-the-art digital cancellation as presented in [10]. The performance realized by this algorithm is significantly limited due to the presence of the SoI, which is impossible to detect due to the excess residual SI. The proposed RLS algorithm offers a significant additional cancellation performance. It can be observed that it achieves the noise floor level with a mean percentage error of $\approx 10\%$. The curve denoted by the RLS, represents the residual SI after subtracting the received SoI from it. The observed cancellation gain between the two algorithms stems from the LMS sub-optimality in the sense that it aims to minimize the mean square error. On the other hand, the RLS goal is to search recursively for the filter weights that minimize the least squares function while exploiting the computed correlation matrix for every sample, which the LMS algorithm ignores.

Finally, the effect of the basis functions transformation is studied, also the case without transformation (w/o Cholesky) was included to show the degradation resulted when not carried out. The observed fluctuations in the PSD behavior occurs due to the large power difference between the p nonlinear components. Thus, leading to a drastic degradation in the cancellation performance.

An additional important KPI is the computational complexity provided by the investigated algorithms. Figure 3, presents the main investigated algorithms along with their cancellation performance, and shows the significant computational burden saved via exploiting the DCD algorithm. RLS-matrix inversion lemma (MIL) represents the conventional RLS based on the

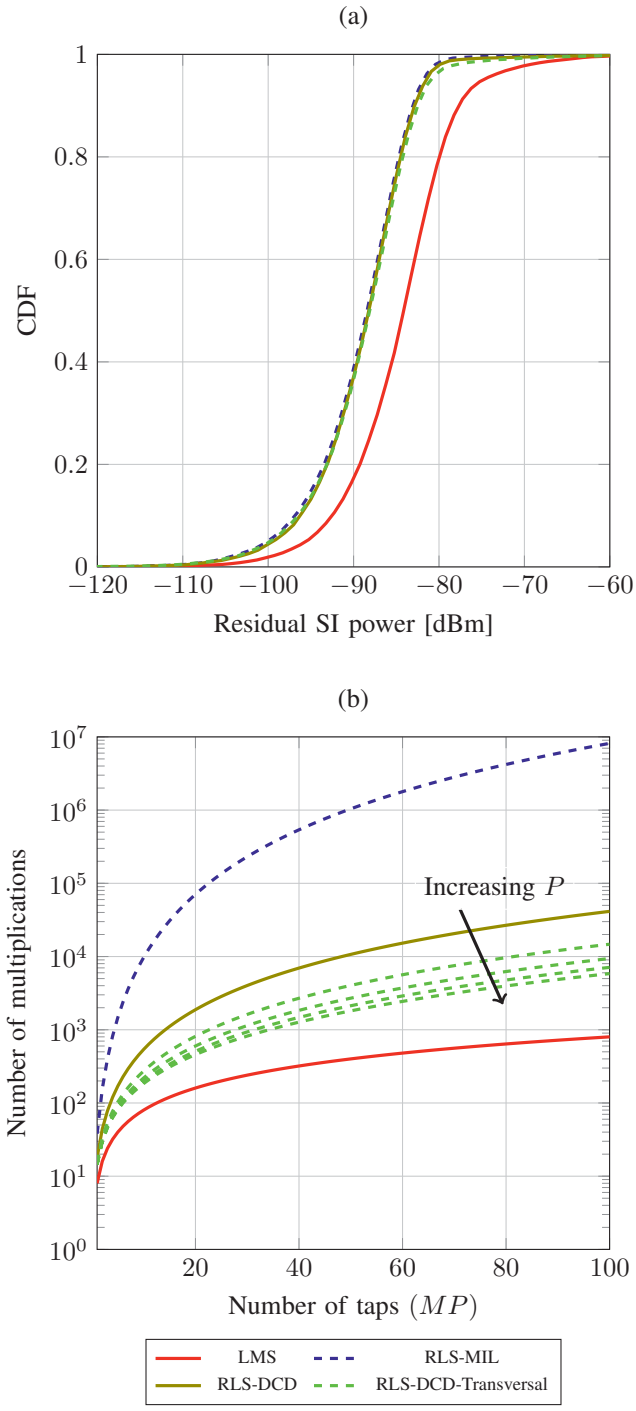

Fig. 3. (a) Cumulative distribution function of residual signal after digital cancellation for different digital cancellation algorithms . (b) Computational complexity comparison as a function of number of filter taps

MIL [19]. It can be observed the gain achieved by the RLS algorithm with the added complexity as a trade off. Additionally, the computational saving provided by the DCD with nearly same cancellation performance, favors it as an alternative to the conventional RLS algorithm. Further savings in the DCD computational complexity can be achieved by

ISBN 978-3-8007-4394-0

exploring the stationarity characteristic of the input data as explained in the previous section.

The green curves show the complexity cost for an increasing set of P of the proposed transversal RLS algorithm. For the dashed green curves, the complexity is now a function of M and P, which are decoupled. For the ease of the visualization, P is fixed for each curve and only M is varied accordingly. Multiple values of P are plotted to show the complexity reduction realized by the transversal RLS algorithm. Furthermore, the performance loss is negligible compared to the savings in the computational complexity. As a result, one can conclude that the computational complexity can be significantly reduced via the DCD algorithm combined with the transversal characteristic of the input data vector.

V. Conclusion

Throughout this work, a low-complexity digital cancellation solution based on a transversal RLS-DCD algorithm was proposed. An enhancement of the cancellation performance was realized, compared to the state-of-the-art solutions. Additionally, a pre-transmission step based on the orthogonalization of the basis functions via Cholesky decomposition was presented, to ensure a higher realized cancellation performance.

The simulation results validated the gain achieved by the proposed algorithm, especially with the existence of a received SoI. The reception is carried out simultaneously while estimating the residual SI signal. A complexity analysis of different cancellation algorithms was presented to show the complexity reduction realized by the proposed algorithm. The cancellation gain realized by the proposed algorithm along with the low computational complexity represents a promising candidate for the design of the digital canceler in full duplex systems.

VI. Acknowledgment

This work was supported by the European Commission in the framework of the H2020-ICT-2014-2 project Flex5Gware (Grant agreement no. 671563).

References

[1] F. Boccardi, R. W. Heath, A. Lozano, T. L. Marzetta, and P. Popovski, "Five Disruptive Technology Directions for 5G," *IEEE Commun. Mag.*, vol. 52, no. 2, pp. 74–80, February 2014.

[2] M. Agiwal, A. Roy, and N. Saxena, "Next Generation 5G Wireless Networks: A Comprehensive Survey," *IEEE Communications Surveys Tutorials*, vol. 18, no. 3, pp. 1617–1655, thirdquarter 2016.

[3] M. Chung, M. S. Sim, J. Kim, D. K. Kim, and C. b. Chae, "Prototyping Real-Time Full Duplex Radios," *IEEE Commun. Mag.*, vol. 53, no. 9, pp. 56–63, September 2015.

[4] A. Sabharwal, P. Schniter, D. Guo, D. W. Bliss, S. Rangarajan, and R. Wichman, "In-Band Full-Duplex Wireless: Challenges and Opportunities," *IEEE J. Sel. Areas Commun.*, vol. 32, no. 9, pp. 1637–1652, Sept 2014.

[5] D. Bharadia, E. McMilin, and S. Katti, "Full Duplex Radios," in *Proceedings of the ACM SIGCOMM 2013 Conference on SIGCOMM*, ser. SIGCOMM '13. New York, NY, USA: ACM, 2013, pp. 375–386. [Online]. Available: http://doi.acm.org/10.1145/2486001.2486033

[6] A. Goldsmith, *Wireless Communications*. New York, NY, USA: Cambridge University Press, 2005.

[7] E. Ahmed and A. M. Eltawil, "All-digital Self-Interference Cancellation Technique for Full-Duplex Systems," *IEEE Trans. Wireless Commun.*, vol. 14, no. 7, pp. 3519–3532, July 2015.

[8] E. Ahmed, A. M. Eltawil, and A. Sabharwal, "Self-interference Cancellation with Nonlinear Distortion Suppression for Full-Duplex Systems," in *2013 Asilomar Conference on Signals, Systems and Computers*, Nov 2013, pp. 1199–1203.

[9] ——, "Self-Interference Cancellation with Phase Noise induced ICI Suppression for Full-Duplex Systems," *CoRR*, vol. abs/1307.4149, 2013. [Online]. Available: http://arxiv.org/abs/1307.4149

[10] D. Korpi, Y. S. Choi, T. Huusari, L. Anttila, S. Talwar, and M. Valkama, "Adaptive Nonlinear Digital Self-interference Cancellation for Mobile Inband Full-Duplex Radio: Algorithms and RF Measurements," in *2015 IEEE Global Communications Conference (GLOBECOM)*, Dec 2015, pp. 1–7.

[11] M. Isaksson, D. Wisell, and D. Ronnow, "A Comparative Analysis of Behavioral Models for RF Power Amplifiers," *IEEE Trans. Microw. Theory Tech.*, vol. 54, no. 1, pp. 348–359, Jan 2006.

[12] L. Ding, G. T. Zhou, D. R. Morgan, Z. Ma, J. S. Kenney, J. Kim, and C. R. Giardina, "A Robust Digital Baseband Predistorter Constructed using Memory Polynomials," *IEEE Trans. Commun.*, vol. 52, no. 1, pp. 159–165, Jan 2004.

[13] B. Razavi, *Design of Analog CMOS Integrated Circuits*, 1st ed. New York, NY, USA: McGraw-Hill, Inc., 2001.

[14] W. J. Rugh, *Nonlinear System Theory : The Volterra/Wiener Approach*, ser. Johns Hopkins series in information sciences and systems. Baltimore: Johns Hopkins University Press, 1981. [Online]. Available: http://opac.inria.fr/record=b1090598

[15] R. Askar, B. Schubert, W. Keusgen, and T. Haustein, "Agile Full-duplex Transceiver: The Concept and Self-Interference Channel Characteristics," in *European Wireless 2016; 22th European Wireless Conference*, May 2016, pp. 1–7.

[16] D. Korpi, T. Riihonen, V. Syrjaelae, L. Anttila, M. Valkama, and R. Wichman, "Full-Duplex Transceiver System Calculations: Analysis of ADC and Linearity Challenges," *IEEE Trans. Wireless Commun.*, vol. 13, no. 7, pp. 3821–3836, July 2014.

[17] D. Korpi, T. Huusari, Y. S. Choi, L. Anttila, S. Talwar, and M. Valkama, "Digital Self-Interference Cancellation under Nonideal RF Components: Advanced Algorithms and Measured Performance," in *2015 IEEE 16th International Workshop on Signal Processing Advances in Wireless Communications (SPAWC)*, June 2015, pp. 286–290.

[18] Y. V. Zakharov, G. P. White, and J. Liu, "Low-Complexity RLS Algorithms Using Dichotomous Coordinate Descent Iterations," *IEEE Trans. Signal Process.*, vol. 56, no. 7, pp. 3150–3161, July 2008.

[19] S. Haykin, *Adaptive Filter Theory (3rd Ed.)*. Upper Saddle River, NJ, USA: Prentice-Hall, Inc., 1996.

[20] G. K. Boray and M. D. Srinath, "Conjugate Gradient Techniques for Adaptive Filtering," *IEEE Trans. Circuits Syst. I*, vol. 39, no. 1, pp. 1–10, Jan 1992.

[21] Y. Zakharov and F. Albu, "Coordinate Descent Iterations in Fast Affine Projection Algorithm," *IEEE Signal Process. Lett.*, vol. 12, no. 5, pp. 353–356, May 2005.

[22] J. He, J. S. Yang, Y. Kim, and A. S. Kim, "System-Level Time-Domain Behavioral Modeling for A Mobile Wimax Transceiver," in *2006 IEEE International Behavioral Modeling and Simulation Workshop*, Sept 2006, pp. 138–143.

